Environ. Chem. **2014**, *11*, 173–180
http://dx.doi.org/10.1071/EN13148

In situ electrochemical method for detecting freely dissolved polycyclic aromatic hydrocarbons in water

Abra Penezić[1]*, Blaženka Gašparović[1], Draženka Stipaničev[2], Andrew Nelson[3]

[1]*Ruđer Bošković Institute, Center for Marine and Environmental Research, POB 180, HR-10002 Zagreb, Croatia*

[2] *180, HR-10002 Zagreb, Croatia*

[3]*Centre for Self Organising Molecular Systems, School of Chemistry, University of Leeds, LS2 9JT Leeds, UK*

Abstract

A new sensing system for polycyclic aromatic hydrocarbons (PAHs) in waters is being developed. The system consists of a wafer-based device with a chip-based mercury on platinum microelectrode as a working electrode and a platinum auxiliary electrode, incorporated into a flow cell system with an external reference electrode. The Hg microelectrode was coated with a phospholipid–triglyceride mixed layer and interactions between anthracene, phenanthrene,
pyrene and fluoranthene and the layer were monitored using rapid cyclic voltammetry. The layer proved sensitive to interactions with PAHs in 'organic matter free' seawater, with respective detection limits of 0.33, 0.35, 0.15 and 0.32 mgL^{-1} for phenanthrene, pyrene, anthracene and fluoranthene. Tested interferences, such as sodium humate, dextran T-500 and bovine serum albumin, representing humic substances, polysaccharides and proteins, did not have an influence on the layer response. The system was also tested with a river water sample where concentrations of PAHs were determined using the standard addition method and compared with the results obtained by using gas chromatography–mass spectrometry (GC-MS). The concentration of total PAHs obtained by the standard addition method is ~80% lower compared with the results obtained by GC-MS analysis. The difference is explained by the fact that the electrochemical method measures water-soluble and free PAHs whereas the chromatographic method measures both dissolved and particulate–organic PAHs.

Introduction

Polycyclic aromatic hydrocarbons (PAHs) are persistent, hydrophobic compounds found in different environmental compartments[1] with their concentrations in aquatic systems ranging from nanograms to micrograms per litre.[2–5] The most significant sources of PAHs include incomplete wood combustion, petroleum products and anthropogenic sources such as steel and petroleum industries.[6,7] More hydrophobic PAHs tend to adsorb and associate with particles, whereas lower molecular weight PAHs, which are less hydrophobic, are more likely to be present in the dissolved form in the aquatic environment, which makes themmore available for uptake by aquatic organisms.[8] Some PAH molecules are carcinogenic whereas some are transformed into carcinogenic and mutagenic compounds during metabolic processes[9] and for these reasons their levels in the aquatic environment should be closely monitored. The traditional methods for determining PAHs in the environment include gas chromatography (GC) and liquid chromatography

(LC) coupled with mass spectrometry (MS).[10]
Although chromatographic methods are accurate and have very low detection limits,[11] they require sample pretreatment and extraction and are therefore time consuming and expensive. This has led to the development of different immunochemical and electrochemical methods[12,13] for PAH detection, lowering the cost and shortening the analysis time in comparison to standard GC and LC procedures. Notwithstanding, these methods can often have complex configurations and binding systems used for detection, making them less user-friendly. A considerable step towards the development and in situ application of simple and rapid methods for the detection of PAHs was made by introducing supported lipid bilayers and monolayers for sensing purposes where a biomembrane active analyte influences the structure of the lipid layers. A lipid-coated Hg electrode is such a supported layer system and the interaction between the analyte and the lipid layer disrupts the organisation of the layer, which can be easily monitored electrochemically by means of rapid cyclic voltammetry (RCV).[14,15] In the case of the lipid-coated Hg device, the applied potential causes sharp discontinuities in the capacitative current–potential traces representing electrically induced phase transitions of the lipid monolayer relating to the switch in the orientation of the polar head groups in the monolayer and nucleation and growth processes.[16,17] While the lipid layer is continuously scanned, the analyte, lipophilic PAH molecules, interacts with the layer and the interaction modifies the form of these phase transitions. A phospholipid monolayer of 1,2-dioleoyl-sn-glycero-3-phosphocholine (DOPC), adsorbed on to a hanging Hg drop electrode (HMDE) has been successfully used for studying interactions with hydrophobic organic compounds[18,19] and for studying ion channel function and electron transfer through the coated layer.[20–22] With the development of Pt–Hg film microelectrodes[23] the Hg–phospholipid system was transferred to a more robust platform rendering it more applicable for screening interactions with membrane active substances,[24] as well as for studying interactions with polymers and nanoparticles.[25,26] Besides being a desirable substrate for studying lipid layers, Hg film electrodes, like the iridium-based Hg film electrode and Hg-coated gold, carbon and silver electrodes, have been investigated for purposes of anodic stripping voltammetry and trace metal detection in seawater.[27,28]
The goal of this study was to develop and test a novel robust and low-cost electrochemical, biomembrane mimicking sensor for PAH detection as an early warning system for the presence of PAH in natural waters. A mixed layer of phospolipid 1-palmitoyl-2-oleoyl-sn-glycero-3-phosphocholine (POPC) and triolein (TG), an oleic acid triglyceride, was used as a model layer. Triglycerides are major constituents of marine mammal's blubber, where pollutants and toxins tend to bioaccumulate,[29] and they are, in particular TG, used as biomimetic adsorbents in assessing PAH uptake, bioavailability and sequestration.[30–32] In vesicles composed of TG and POPC, lipids are organised in such a way that the headgroups have restricted mobility compared with vesicles composed only of POPC, but the mobility of the acyl chain region is increased.[33] Khandelia et al.[34] also report the possible existence of mobile neutral lipid aggregates in a mixed lipid layer of POPC and TG. Thus, in this work a

mixed lipid layer of POPC and TG was chosen, rather than a single lipid layer, as a sensing platform more susceptible to interaction with hydrophobic molecules, such as PAHs. In this paper the sensor was tested for the determination of four PAH compounds, namely phenanthrene, anthracene, pyrene and fluoranthene, which have been identified by the United States Environmental Protection Agency (EPA) as particularly important because of their toxicity to mammals and aquatic organisms. The influence of different model organic molecules occurring in natural waters, such as humic substances, proteins and polysaccharides have been evaluated as possible interfering compounds on the supported layer detection of selected PAHs. Finally, the performance of the system was characterised on a natural river water sample with the aim of comparing the sensitivity of the electrochemical sensor with the conventional GC-MS method of PAH determination in natural samples.

Experimental

Mercury film electrodes and the flow cell system

The working electrode in our sensor was a mercury film electrodeposited on to platinum discs.[23] As described in our earlier work,[24] the Pt/Hg film electrodes are part of a silicon wafer-based microdevice that contains eight working electrodes, each with a radius of 500 mm, of which only one is addressed during measurement, and a platinum counter electrode. Hg film microelectrodes were made by chronocoulometric electrodeposition of Hg on to Pt discs on the wafer, using an open top standard three electrode cell with an external Ag/AgCl reference electrode (3 mol L^{-1} KCl inner filling, 0.1 mol L^{-1} perchloric acid outer filling) and a platinum bar counter electrode.[23] The wafer-based device with the Hg film working electrodes and a Pt counter electrode was incorporated into a flow cell with an external RedRod reference electrode (E=0.194V *v.* standard hydrogen electrode, SHE). The flow cell was a part of a semiautomated analysis system. The Hg film electrode capacitative current was measured byRCV at ramp rates.10Vs^{-1}, using an Ivium Compactstat potentiostat (Ivium Technologies, Eindhoven, the Netherlands) coupled with Powerlab 4/26 signal generator (ADInstruments, Sydney, Australia). RCV was also used for characterising the lipid layer coated on the surface of the electrode as well as the interactions between the lipid layer and analytes. In the absence of electroactive species such as O_2, which was achieved by deaerating the sample solution, the RCV current is linearly related to the capacitance of the electrode–electrolyte interface.The flow of the electrolyte and the samples through the cell was controlled using a Bio-Chem Valve solenoid-operated isolation valve (Bio Chem Fluidics, Boonton, NJ, USA) and an Ismatec peristaltic pump (Wertheim, Germany) with tygon and PTFE peristaltic tubing. The flow was set to 5mL min-1. The electrolyte used was 0.5 mol L^{-1} NaCl, buffered with $NaHCO_3$ (Sigma–Aldrich, St Louis, MO, USA) to pH 8.1. The electrolyte was prepared with ultra pure water (Direct–Q, Millipore system, Billerica, MA, USA) and NaCl calcined at 450 8C for 4 h and purified with activated charcoal in order to remove residual traces of organic matter, including organic contaminants, before use. ‘Organic matter free’ seawater

('OM free' seawater) was prepared by filtering seawater through a 0.7-mm pore size GF/F filter (Whatman, Maidstone, UK) and UV irradiating for 24 h (150-W mercury lamp, Hanau, Germany), after which activated charcoal was added in order to remove residual traces of organic matter, and kept in the seaswater overnight before final filtration and use. The residual amount of dissolved organic carbon (DOC) was 0.03 mg L^{-1}. As seawater is naturally buffered, no extra buffer was added to it. For river water analyses, a saturated solution of NaCl was added to the otherwise untreated river sample before analysis, to obtain a 0.5-mol L^{-1} NaCl solution of the sample.

Lipid dispersion, coating of the electrode, analysis procedure

1-Palmitoyl-2-oleoyl-sn-glicero-3-phosphocholine (POPC) (Sigma–Aldrich), and an oleic acid triglyceride, triolein (TG) (Sigma–Aldrich) were mixed in a 3 : 1 molar ratio, as a chloroform stock solution. Chloroform was removed under nitrogen flow and a 0.5 mol L^{-1} NaCl solution was added to the dried lipid mixture, after which the solution was shaken for,4 h using a laboratory shaker, giving a 1.3 mmol L^{-1} dispersion of POPC and TG. Such a dispersion contained lipid vesicles without defined liposome lamella thickness. The size distribution of the liposomes was measured using a Zetasizer Nano ZS equipped with a green laser (532 nm). The intensity of scattered light was detected at an angle of 1738. All data processing was done using *Zetasizer software 6.20* (Malvern Instruments, Malvern, UK).

Table 1. Chemical properties of analysed polycyclic aromatic hydrocarbons
Recommended log K_{ow} values of octanol–water partition coefficients from LOGKOW databank of evaluated octanol–water coefficients

Common name	Molecular structure	Number of rings	Water solubility ($\mu g\ L^{-1}$ at 25 °C)	Seawater solubility ($\mu g\ L^{-1}$ at 25 °C)	log K_{ow}
phenanthrene	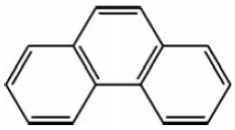	3	1002[36]	663[36]	4.5
anthracene	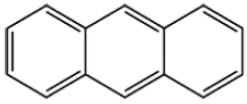	3	75[37]	31[36]	4.5
pyrene	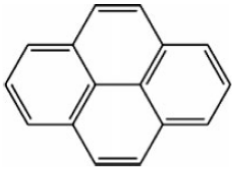	4	135[38]	86[36]	5.0
fluoranthene	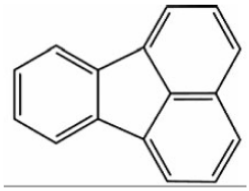	4	265[37]	data not found	5.2

To coat the Hg film electrode, the dispersion of lipids was injected into the electrolyte flow by a switch operated by a Bio-Chem Valve micro pump (Bio Chem Fluidics, Boonton, NJ, USA) where it passed through the flow cell while performing RCV scans from the potential at which the layer was adsorbed to the potential where complete desorption occurred (-0.4 to -3.0 V). These cyclic scans caused the disruption of vesicles in the fluctuating high electric field and polarised the electrode surface, enabling the adsorption of an organised lipid layer on to the electrode. The adsorption process is described by Hellberg et al.[35] Once the lipids adsorbed on to the surface of the electrode, the scan range was set from -0.38 to -1.16V with a scan rate of $34.4 Vs^{-1}$. The layer was continuously scanned for 100 scans (107 s) in order for it to stabilise and to let the excess lipid material flush out of the cell. Subsequently the blank solution (buffered electrolyte or 'OM free' seawater) was passed through the cell for 600 scans (644 s) to record a control cyclic voltammogram. After the blank was analysed, the procedure was repeated with the PAH-spiked, buffered electrolyte or the 'OMfree' seawater sample, which was passed through the flow cell and the interaction between the analyte and the adsorbed mixed lipid layer was monitored in real time. The measurements were carried out in duplicate or triplicate. Stock solutions of all PAHs analysed were prepared in methanol, after which an aliquot was added to the buffered electrolyte or 'OM free' seawater. The concentration of methanol in every sample was kept the same ($0.78 g L^{-1}$) while the concentration of the PAHs in the solution changed. Experiments were conducted to check whether methanol influences the mixed lipid layer at the concentration present in the sample. A 0.5-mol L^{-1} NaCl solution, pH 8.1, containing $0.78 g L^{-1}$ of methanol was passed through the flow cell and was shown to have no influence on the capacitance current peaks of the layer. From this we concluded that methanol did not affect the layer at this concentration. After the analysis, the Hg film electrode was cleaned by applying a RCV scan in the same potential range as for adsorption of the lipid layer. Selected PAHs were determined in the concentration range from 0.25 to 1.5 mgL^{-1}, with a $0.25 mgL^{-1}$ concentration step increase. Phenanthrene, anthracene, pyrene and fluoranthene have an octanol–water partition coefficient between 4.5 and 5.2, as such their water solubility is relatively high compared with other PAHs with higher molecular weight and they are composed of three and four benzene rings with the exception of fluoranthene, which consists of three benzene rings connected by a five-membered ring (Table 1, solubility data was taken from the literature[36–38]). In order to assess the cumulative effect of a mixture of PAHs on the characteristics of the capacitance peaks of the POPC–TG mixed lipid layer, stock solutions of phenathrene and pyrene in a 1 : 1 ratio, prepared in methanol, were used. The summed concentrations of pyrene and phenanthrene in the samples analysed ranged from 0.5 to 3 mgL^{-1}. Interferences tested were organic molecules commonly present in natural waters such as humic substances, proteins and polysaccharides. Examples of these interfering compounds included Na-humate (Aldrich Chemie), carbohydrate, dextrane T-500 (Sigma Aldrich) and protein, bovine serum albumin (Sigma Aldrich), all prepared as 'OM free' seawater solutions. The repeatability of the method was tested by measuring 10 samples of electrolyte spiked with the same concentration of pyrene.

Analysis of the PAHs

Standard PAHs, naphthalene, methyl-naphthalene, dimethylnaphthalene, acenaphthylene, acenaphthene, fluorene, phenanthrene, anthracene, fluoranthene, pyrene, chrysene, benzo[*a*] anthracene, benzo[*b*]fluoranthene, benzo[*k*]fluoranthene, benzo [*a*]pyrene, benzo[*g*,*h*,*i*]perylene, dibenzo[*a*,*h*]anthracene and indeno[1,2,3-*cd*]pyrene were obtained in a mixture (each at 2000 mgmL^{-1}) from Supelco (Bellefonte, PA, USA). Deuterated internal standards (naphthalene-d_8, acenaphthene-d_{10}, phenanthrene-d_{10} and chrysene-d_{12}) were obtained from Sigma–Aldrich. Working standards of PAHs were prepared by combining the standard mixture with the corresponding internal standard stock solution. These solutions were further diluted with dichloromethane for the preparation of calibration solutions in the range of 1–250 ngmL^{-1}. All solvents (dichloromethane, ethyl acetate, acetone, hexane and methanol) used for sample processing and analyses were Pesticide & GC residue grade, free of analytes (PAH) and interferences, obtained from Labscan (Gliwice, Poland). All glassware, including sampling bottles, were cleaned with ultra pure water, methanol and acetone, before use. Water samples were collected in amber glass bottles and acidified. The bottles were covered with screw caps and were immediately transported to the laboratory after sampling for analysis. After returning to the laboratory, samples (1.0 L) were processed on automated sample handling equipment manufactured by Horizon Technology, Inc. made of (i) the Automated Extraction System SPE-DEX 4790, (ii) the Envision Platform Controller and (iii) the DryVap Automated Drying and Concentration System. The Atlantic C18 solid phase extraction disc was used for solid phase extraction (SPE). The SPE-DEX 4790 Extractor processed 1 L of surface water sample directly from the original sample bottle. It automatically delivered all solvents, regulated sample processing, including disc soak and drying times, rinsed the sample bottle and collected the final extract before concentration. The final extract was then concentrated by evaporation under nitrogen gas in a DryVapAutomated Drying and Concentration System, and then adjusted to a volume of 1mL with dichloromethane after adding the internal standards. The final volume of 1mL of extracts in dichloromethane were then analysed by GC-MS.The structures of the PAHs were confirmed by GC-MS selective ion monitoring on a GC-MS QP 2010 Plus (Shimadzu, Japan). A fused-silica Elite-5MS capillary column (60m _0.25-mm internal diameter, 0.25 mm film thickness) was used. Helium with a purity of 99.999% was used as a carrier gas at a column flow rate of 1.67 mLmin^{-1}.
The oven temperaturewas programmed from 40 ºC (holding time 4 min) to 130 ºC at 45 ºC min-1, to 180 C at 12ºC min^{-1}, to 240 ºC at 7 ºC min^{-1} and to 320 C at 8ºC min^{-1}. A 25-mL volume was injected in LVI-PTV mode (large volume injection–programmable temperature vaporising inlet mode). The mass spectrometer was operated in the electron impact (EI) mode with an ion source at 200 ºC and interface temperature at 250 ºC, the EI energy was set at 70 eV. Identification of the PAH compounds was performed by comparing GC retention time, mass spectra and ratios of target and qualifier ions with those of authentic standards. Quantification of individual compounds was based on comparison of peak areas with those of the recovery standards. Verification of accuracy and precision for GC-MS methods followed

the Environmental Protection Agency (EPA) method described by the United States EPA Method 8270.[39] Before sample analysis, relevant standards were analysed to check column performance, peak height and resolution and limits of detection. With each set of samples to be analysed, a solvent blank, a standard mixture and a procedural blank were run in sequence to check for contamination, peak identification and quantification.

Results and discussion

The size of the liposomes in the POPC–TG lipid dispersion for coating the Hg electrode was determined by using the size distribution by number. A total of 98% of the vesicles in the dispersion were between 89 and 134 nm in diameter, whereas the remaining 2% were between 671 and 1075 nm in diameter (Fig. 1). The interactions between the layer and the analytes were reproducible, leading to the conclusion that the eventual variation in size of the liposomes present in the dispersion used for coating the electrode did not affect the coating process. The capacitive current–potential trace of the POPC–TG mixed lipid layer (Fig. 2) shows the presence of two capacitance peaks, representing phase transitions of the adsorbed layer.

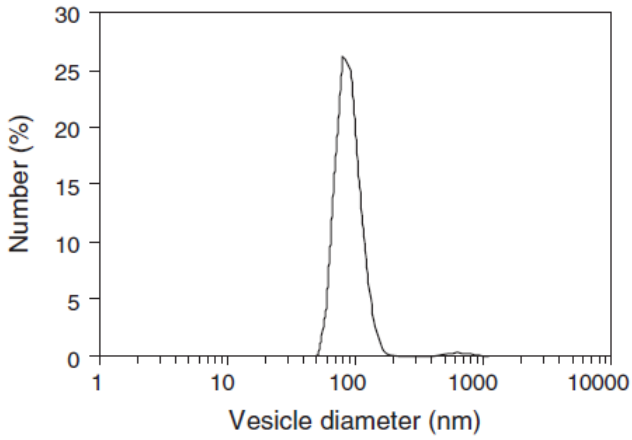

Fig. 1. Size distribution of vesicles in the 1-palmitoyl-2-oleoylsn-glycero-3-phosphocholine–triolein lipid dispersion determined by using the size distribution by number.

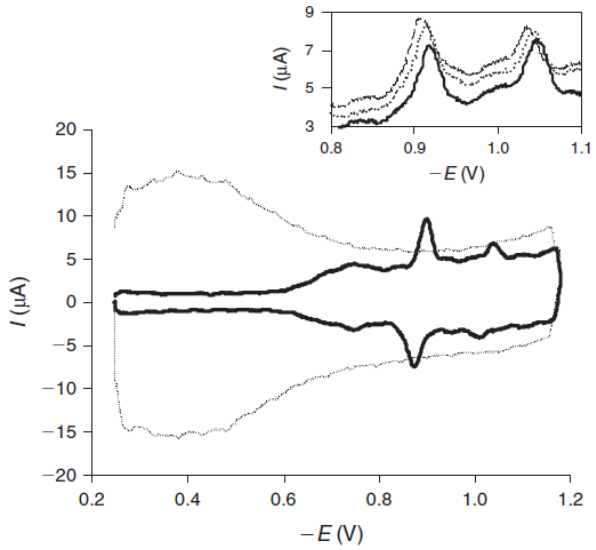

Fig. 2. Flow cell rapid cyclic voltammetry scans of a clean Hg film electrode (dotted line) and 1-palmitoyl-2-oleoyl-sn-glycero-3-phosphocholine–triolein 3 : 1 molar ratio mixed lipid layer coated Hg film electrode (solid line), showing two distinct capacitance current peaks at *E*L'_0.9 and-1.04 V. Inset: the capacitance peaks before (dashed line) and after a buffered electrolyte (0.5 mol L-1 NaCl, pH 8.1) spiked with 0.75 and 1.5 mgL-1 phenanthrene has been passed through the flow cell for 644 s (dotted and solid line respectively).

The inset of Fig. 2 shows a shift in the potential of the capacitance peaks to more negative values after a buffered electrolyte spiked with 0.75 and 1.5 mgL^{-1} phenanthrene was passed through the flow cell for 600 continuous scanning cycles. The shift in the potential of the POPC–TG mixed lipid layer capacitance peaks caused by the interaction with the PAH molecules analysed was observed for both peaks, but the second, more negative capacitance peak, was more sensitive to the presence of the analyte and a linear relation was determined between the concentration of the analyte passed through the flow cell and the shift of the potential of the capacitance peak. Therefore, only the second peak was considered as an indicator of the analyte–POPC–TG mixed lipid layer interaction and was used for constructing the calibration curve plots for the determined PAHs. The relative standard deviation of repeatability was 8.06 %.

Calibrations

The measurements for constructing the first calibration curves were carried out with samples of 0.5 mol L^{-1} NaCl, buffered to pH 8.1 and spiked with phenanthrene, anthracene, pyrene and fluoranthene. To obtain calibration curves in buffered electrolyte, the four PAHs were added separately to the buffered electrolyte, after which the solutions were passed through the flow cell while performing RCV.

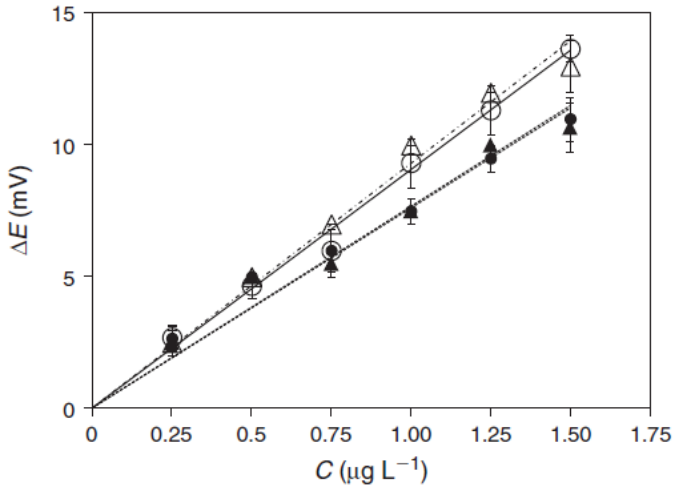

Fig. 3. Calibration curves for phenanthrene (white circle, solid line), anthracene (white triangle, intermittent line) pyrene (black circle, dotted line) and fluoranthene (black triangle, dotted line) in 0.5 mol L^{-1} NaCl, pH 8.1 (*C*, concentration), constructed by measuring the peak potential shift of the second capacitance peak of the 1-palmitoyl-2-oleoyl-sn-glycero-3-phosphocholine–triolein mixed lipid layer.

All four PAHs caused a negative shift in the potential of the second capacitance peak of the POPC–TG mixed lipid layer and a linear relationship was observed between the increase of the concentration of the PAH and the shift of the peak's potential (Fig. 3). The detection limits were calculated using the standard error of the linear regression curve (Table 2). The slopes of the calibration curves for phenanthrene and anthracene were slightly higher than those for pyrene and anthracene, which suggests that the POPC–TG mixed lipid layer in buffered electrolyte has a slightly higher affinity for three-ring PAHs. For the second set of calibration curves; anthracene, phenanthrene, pyrene and fluoranthene were separately added to 'OM free' seawater and tested for interaction with the POPC–TG mixed lipid layer. Obtaining calibration curves for selected PAHs in 'OM free' seawater first required testing the influence of the pure 'OM free' seawater on the POPC–TG mixed lipid layer. It has been shown previously that seawater has an influence on phospholipid monolayers,[40] where a shift in the potential of the capacitance peaks of DOPC layers was observed and attributed to magnesium and calcium ions present in seawater. We found that pure 'OM free' seawater has an effect on the capacitance peaks of the POPC–TG mixed lipid layer, seen as a shift of the first peak to more negative potentials, whereas the second peak shifted towards more positive potentials (Fig. 4). This influence did not, however, affect the interaction between PAHs in the spiked 'OM free' seawater and the POPC–TG mixed lipid layer.

Phenanthrene, anthracene, pyrene and fluoranthene in 'OM free' seawater all interacted with the POPC–TG mixed lipid layer, and in order to construct the calibration curves, the influence of the pure 'OM free' seawater was subtracted from the influence of the PAH spiked 'OM free' seawater. The interaction of the analysed PAHs with the POPC–TG mixed lipid layer caused a negative shift of the potential of the second

capacitance peak (Fig. 5). The regression equations and detection limits are given in Table 2. In order to assess the cumulative effect of a mixture of PAHs on the potentials of the capacitance peak of the POPC–TG mixed lipid layer, 'OM free' seawater was spiked with mixtures of pyrene and phenanthrene. The mixture of pyrene and phenanthrene interacted with the mixed lipid layer and a negative shift in the potential of the second capacitance peak was observed. The shifts in the potentials of the second capacitance peaks caused by pyrene and phenanthrene in 'OM free' seawater analysed separately were summed in order to obtain calculated values for the cumulative influence

Table 2. Regression equations and detection limits for the polycyclic aromatic hydrocarbons (PAHs) anthracene, phenanthrene,pyrene and fluoranthene in 0.5 molL^{-1} NaCl, buffered to pH 8.1, and 'organic matter (OM) free' seawater

PAH	Regression equation	Detection limit (μg L^{-1})
0.5 mol L^{-1} NaCl, buffered to pH 8.1		
anthracene	$\Delta V = 8.74 \times [\text{phenanthrene}] + 0.6$ ($R^2 = 0.985$)	0.19
phenanthrene	$\Delta V = 9.98 \times [\text{phenanthrene}] - 0.13$ ($R^2 = 0.477$)	0.26
pyrene	$\Delta V = 6.47 \times [\text{pyrene}] + 1.27$ ($R^2 = 0.991$)	0.14
fluoranthene	$\Delta V = 6.61 \times [\text{fluoranthene}] + 1.07$ ($R^2 = 0.973$)	0.26
'OM free' seawater		
anthracene	$\Delta V = 7.58 \times [\text{anthracene}] + 0.35$ ($R^2 = 0.991$)	0.15
phenanthrene	$\Delta V = 7.46 \times [\text{phenanthrene}] + 0.57$ ($R^2 = 0.957$)	0.33
pyrene	$\Delta V = 6.51 \times [\text{pyrene}] + 0.47$ ($R^2 = 0.95$)	0.35
fluoranthene	$\Delta V = 7.54 \times [\text{fluoranthene}] - 0.26$ ($R^2 = 0.959$)	0.32

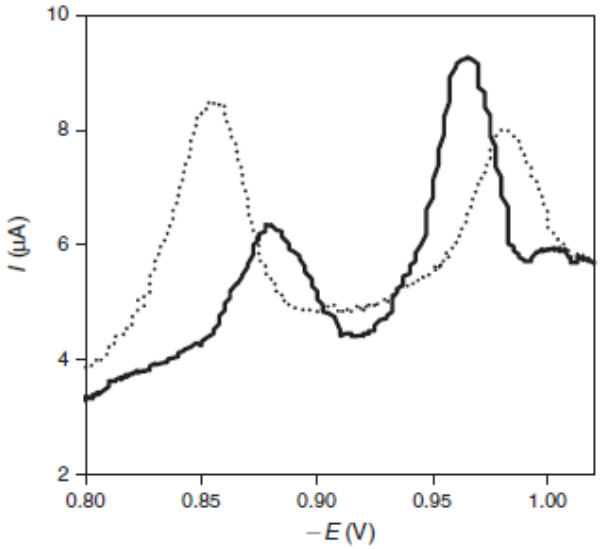

Fig. 4. Shift of the potential of the 1-palmitoyl-2-oleoyl-sn-glycero-3-phosphocholine–triolein mixed lipid layer capacitance peaks (dotted line) after interaction with 'organic matter free' seawater (solid line).

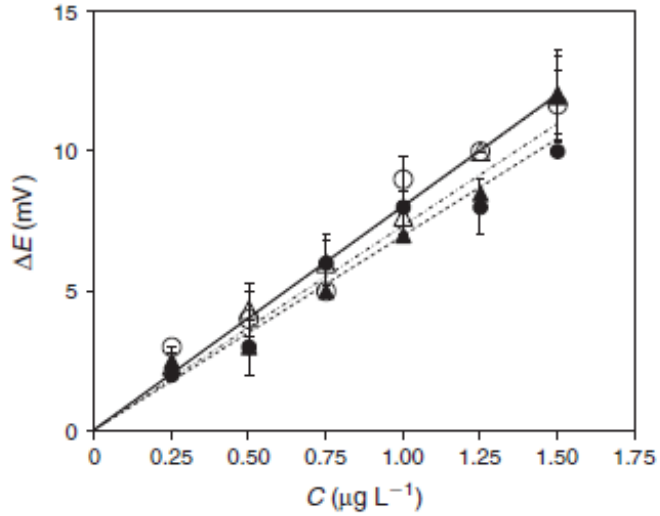

Fig. 5. Calibration curves for phenanthrene (white circle, solid line), anthracene (white triangle, dotted line) pyrene (black circle, dashed line) and fluoranthene (black triangle, intermittent line) spiked 'organic matter free' seawater, constructed by measuring the peak potential shift of the second capacitance peak of the 1-palmitoyl-2-oleoyl-sn-glycero-3-phosphocholine–triolein mixed lipid layer (*C*, concentration).

of these two compounds. The summed results were compared with the shifts in the potentials of the capacitance peaks caused by the analysed mixture of pyrene and phenanthrene in 'OM free' seawater (Fig. 6). The measured and the calculated values of the shifts in the potentials of the capacitance peaks are in good agreement, which would suggest that the cumulative effect of the PAHs affecting the layer can be compared with the sum of individual PAHs affecting the layer separately. This would enable us to detect the sum of all PAHs that affect the mixed lipid layer, present in a sample.

Interferences

In order to determine PAHs in real samples, it is important to consider the possible influence of interfering substances that are naturally occurring in waters, such as humic substances, polysacharides and proteins. 'OM free' seawater was therefore separately spiked with sodium humate (1 mg L^{-1}), dextranT-500 (3 mg L^{-1}) and bovine serum albumin (1 mg L^{-1}) and tested to check if these compounds would influence the POPC–TG mixed lipid layer.

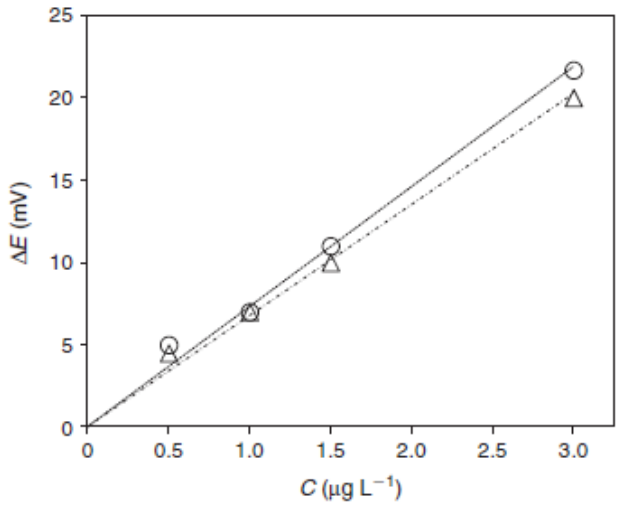

Fig. 6. The sum of separate influences of pyrene and phenanthrene in spiked 'organic matter (OM) free' seawater on the 1-palmitoyl-2-oleoyl-snglycero-3-phosphocholine–triolein mixed lipid layer (white circle, dotted line) and influence of the mixture of pyrene and phenanthrene spiked 'OM free' seawater on the POPC–TG mixed lipid layer (white triangle, intermittent line) (*C*, concentration).

The concentrations of the compounds were selected so as to exceed concentrations usually found in natural samples. Sodium humate, dextran T-500 and bovine serum albumin did not induce a shift of the potentials of capacitance peaks of the mixed lipid layer, so it was concluded that none of the tested compounds interacted with the mixed lipid layer for the concentrations analysed.

Testing the system

To intercalibrate the system with an established analytical method, a sample from the Sava River, passing through the capital of Croatia, was analysed to estimate the concentration of the PAHs present, using the sensor with a standard addition method. The total PAH concentration in the sample, including dissolved PAHs as well as PAHs adsorbed and bound to particles and organic substances, were previously determined by GC-MS, and these data are given in Table 3. As determined by GC-MS, the total PAH concentration in this sample was 0.646 mgL^{-1}, and concentrations of pyrene and phenanthrene were 0.020 and 0.166 mgL^{-1}. The standard addition method was used when analysing the samples with the flow cell system because the matrix effect prevented direct determination. The PAHs used for the standard addition method were pyrene and phenanthrene, and the total concentration of PAHs in the sample was determined as the point where the extrapolated line crosses the concentration (x) axis. When standard additions of pyrene were added to the river samples, the estimated total concentration of PAH in the sample was found to be 0.11 mgL^{-1}, and with standard additions of phenanthrene, the total concentration of PAH was estimated to be 0.13 mgL^{-1} (Fig. 7). The difference between the results obtained by GC-MS and by the electrochemical

standard addition method is explained by the fact that the electrochemical method measures water-soluble and free PAHs whereas the chromatographic method measures all PAHs present in the sample, including that dissolved and partitioned with particles or organics. PAHs tend to adsorb to organic particles and bind to humic substances,[41] which causes a decrease in their concentration in the water column and affects their bioavailability.[8,42]

Table 3. Polycyclic aromatic hydrocarbon (PAH) concentration data in the Sava River sample determined by gas chromatography]mass spectrometry

log K_{ow} data are recommended values of octanol–water partition coefficient from log K_{ow} databank of evaluated octanol–water coefficients. Phenanthrene, anthracene, pyrene and fluoranthene are the PAHs whose determination using the electrochemical sensor is described in this paper

PAH	log K_{ow}	C (μg L^{-1})
Naphthalene	3.35	0.00237
2-Methylnaphthalene	4	0.03795
1-Methylnaphthalene	3.87	0.01965
Acenaphtylene	3.61	–
Acenaphthene	3.92	–
Flourene	4.18	0.02762
Phenanthrene	4.52	0.16628
Anthracene	4.5	0.02504
Pyrene	5	0.02052
Fluoranthene	5.2	0.08458
Benz(*a*)anthracene	5.91	0.00302
Chrysene	5.86	0.01264
Benzo(*k*)fluoranthene	6.11	–
Benzo(*b*)fluoranthene	5.78	–
Benzo(*a*)pyrene	6.35	0.12136
Benzo(*ghi*)perylene	6.9	0.05193
Dibenz(*a*,*h*)anthracene	6.75	0.07312
Indeno(1,2,3-*cd*)pyrene	6.3	–

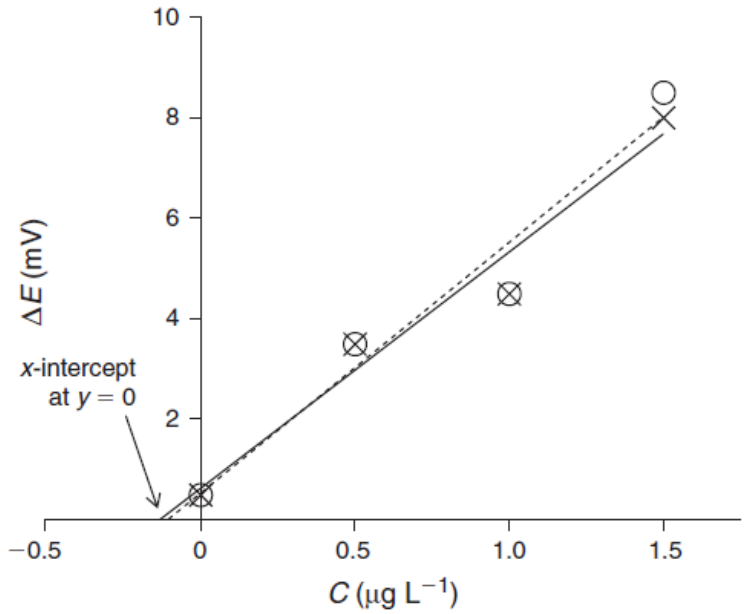

Fig. 7. Standard addition method for determining total polycyclic aromatic hydrocarbon (PAH) concentration in a river sample. Standard additions of pyrene (O) and phenanthrene (X) were used and the total concentration of PAHs was determined as the point where the extrapolated line (dotted line, pyrene; solid line, phenanthrene) crosses the concentration axis (*C*, concentration).

Also, it has been shown previously that the presence of humic substances decreases the influence of PAH on a DOPC monolayer-coated Hg electrode.[40] In order to see the influence of humic substances on the interaction between PAHs and the POPC–TG layer, a 1-mg L^{-1} solution of sodium humate in 'OM free' seawater was spiked with 1.5 mgL^{-1} pyrene, and the shift in the potential of the capacitance peak was measured as 2.5 ± 0.5 mV (0.30 ± 0.07 mgL^{-1} pyrene). Comparison of the potential shifts of the 'OM free' seawater spiked with 1.5 mgL^{-1} pyrene in the presence and absence of sodium humate has shown that there is 74–84% decrease in the influence of the pyrene on the layer when sodium humate is present in the solution. As it has already been shown, the sodium humate alone does not have an influence on the POPC–TG lipid layer, meaning that the decrease of the influence of pyrene is caused by a fraction of pyrene interacting with sodium humate present in the solution, leaving only unbound pyrene to interact with the layer. This would mean that a fraction of the PAHs was adsorbed on to organic particles or bound to organic compounds present in the river sample, leaving unbound, i.e. dissolved PAH, available for detection by the electrochemical sensor.

Conclusion

It has been shown that a wafer-based device containing aHg film microelectrode can be incorporated into a flow cell and used as a platform for supporting mixed lipid layers. This system was successfully used in studying POPC–TG mixed lipid layer–PAH interactions, which led to the construction of calibration curves for phenanthrene, anthracene, pyrene and fluoranthene in buffered 0.5 mol L^{-1} NaCl, with detection limits of 0.26, 0.19, 0.14 and 0.26 mgL^{-1} and detection limits in 'OM free' seawater of 0.33, 0.15, 0.35, and 0.32 mgL^{-1}. Model compounds for naturally occurring organic substances in seawater (humic substances, polysaccharides and proteins) did not have an effect on the capacitance current–potential curves of the mixed lipid layer. In spite of the fact that PAHs are known to adsorb on to organic particles and bind to humic substances, it was possible to detect pyrene in solution in the presence of particulate and dissolved organic material. This leads us to the conclusion that other unbound PAHs could also possibly be detected with the sensor in the presence of particulate and dissolved organic material, and indicates that the system is capable of detecting unbound PAH in aquatic samples. To lower the limits of detection, which would enable the use of the system as a monitoring tool, further modifications of the system and experimental conditions are being carried out.

Acknowledgements

Funding for this work was provided by the Croatian Ministry of Science, Education and Sports, project number 098-0982934-2717 and North Atlantic Treaty Organisation (NATO) Science for Peace (SfP) Award Reference 983147. The authors thank Dr Darija Jurašin for liposome size distribution measurements.

[1] F. Castelli, V. Librando, M. G. Sarpietro, A calorimetric evidence of the interaction and transport of environmentally carcinogenic compounds through biomembranes. *Thermochim. Acta* **2001**, *373*, 133. doi:10.1016/S0040-6031(01)00477-4
[2] J. Dachs, J. M. Bayona, C. Raoux, J. Albaiges, Spatial, vertical distribution and budget of polycyclic aromatic hydrocarbons in the western Mediterranean seawater. *Environ. Sci. Technol.* **1997**, *31*, 682. doi:10.1021/ES960233J
[3] G. C. Cripps, The extent of hydrocarbon contamination in the marineenvironment from a research station in the Antarctic. *Mar. Pollut. Bull.* **1992**, *25*, 288. doi:10.1016/0025-326X(92)90684-X
[4] Y. L. Wu, X. H. Wang, Y. Y. Li, H. S. Hong, Occurrence of polycyclic aromatic hydrocarbons (PAHs) in seawater from the Western Taiwan Strait, China. *Mar. Pollut. Bull.* **2011**, *63*, 459. doi:10.1016/J.MARPOLBUL.2011.03.008
[5] R. J. Law, V. J. Dawes, R. J. Woodhead, P. Matthiessen, Polycyclic aromatic hydrocarbons (PAH) in seawater around England and Wales. *Mar. Pollut. Bull.* **1997**, *34*, 306. doi:10.1016/S0025-326X(96)00096-3
[6] J. S. Latimer, J. Zheng, The sources, transport, and fate of PAHs in the marine environment, in *PAHs: An Ecotoxicological Perspective* (Ed. P.E.T. Douben) 2003, pp. 9–33 (Wiley: Chichester, UK).

[7] R. Eisler, *Polycyclic aromatic hydrocarbon hazards to fish, wildlife, and invertebrates: a synoptic review. Biological Report 85(1.11), Contaminant Hazard Reviews Report number 11* 1987 (US Fish and Wildlife Service, Patuxent Wildlife Research Center: Laurel, MD).
[8] J. Akkanen, A. Tuikka, J. V. K. Kukkonen, On the borderline of dissolved and particulate organic matter: partitioning and bioavailability of polycyclic aromatic hydrocarbons. *Ecotoxicol. Environ. Saf.*

2012, *78*, 91. doi:10.1016/J.ECOENV.2011.11.010
[9] P. E. T. Douben, Introduction, in *PAHs: An Ecotoxicological Perspective* (Ed. P.E.T. Douben) 2003, pp. 3–6 (Wiley: Chichester, UK).
[10] D. L. Poster, M. M. Schantz, L. C. Sander, S. A. Wise, Analysis of polycyclic aromatic hydrocarbons (PAHs) in environmental samples: a critical review of gas chromatographic (GC) methods. *Anal. Bioanal. Chem.* **2006**, *386*, 859. doi:10.1007/S00216-006-0771-0
[11] J. P. Ma, R. H. Xiao, J. H. Li, J. B. Yu, Y. Q. Zhang, L. X. Chen, Determination of 16 polycyclic aromatic hydrocarbons in environmental water samples by solid-phase extraction using multi-walled carbon nanotubes as adsorbent coupled with gas chromatographymass spectrometry. *J. Chromatogr. A* **2010**, *1217*, 5462. doi:10.1016/J.CHROMA.2010.06.060
[12] K. Li, L. A. Woodward, A. E. Karu, Q. X. Li, Immunochemical detection of polycyclic aromatic hydrocarbons and 1-hydroxypyrene in water and sediment samples. *Anal. Chim. Acta* **2000**, *419*, 1. doi:10.1016/S0003-2670(00)00989-2
[13] Y. Y. Lin, G. D. Liu, C. M. Wai, Y. H. Lin, Magnetic beads-based bioelectrochemical immunoassay of polycyclic aromatic hydrocarbons. *Electrochem. Commun.* **2007**, *9*, 1547. doi:10.1016/J.ELECOM.2007.02.007
[14] A. Nelson, Penetration of mercury-adsorbed phospholipid monolayers by polynuclear aromatic-hydrocarbons. *Anal. Chim. Acta* **1987**, *194*, 139. doi:10.1016/S0003-2670(00)84767-4
[15] A. Nelson, N. Auffret, Phospholipid Monolayers of di-oleoyl lecithin at the mercury–water interface. *J. Electroanal. Chem.* **1988**, *244*, 99. doi:10.1016/0022-0728(88)80098-6
[16] A. Nelson, Electrochemical analysis of a phospholipid phase transition. *J. Electroanal. Chem.* **2007**, *601*, 83. doi:10.1016/J.JELECHEM.2006.10.026
[17] A. Nelson, F. A. M. Leermakers, Substrate-induced structural-changes in electrode-adsorbed lipid layers – experimental-evidence from the behavior of phospholipid layers on the mercury–water interface. *J. Electroanal.Chem.* **1990**, *278*, 73. doi:10.1016/0022-0728(90)85124-N
[18] A. Nelson, N. Auffret, J. Borlakoglu, Interaction of hydrophobic organic-compounds with mercury adsorbed dioleoylphosphatidylcholine monolayers. *Biochim. Biophys. Acta* **1990**, *1021*, 205. doi:10.1016/0005-2736(90)90035-M
[19] R. Stoodley, J. Shepherd, K. M. Wasan, D. Bizzotto, Amphotericin B interactions with a DOPC monolayer. Electrochemical investigations. *BBA – Biomembranes* **2002**, *1564*, 289. doi:10.1016/S0005-2736(02)00463-7
[20] A. Nelson, Conducting gramicidin channel activity in phospholipid monolayers. *Biophys. J.* **2001**, *80*, 2694. doi:10.1016/S0006-3495(01)76238-8
[21] A. Nelson, N. Auffret, Phospholipid monolayers of di-oleoyl lecithin (Di-O-Pc) at the mercury–water interface – effects on faradaic reactions. *J. Electroanal. Chem.* **1988**, *248*, 167. doi:10.1016/0022-0728(88)85159-3
[22] A. Nelson, A. Benton, Phospholipid monolayers at the mercury–water interface. *J. Electroanal. Chem.* **1986**, *202*, 253. doi:10.1016/0022-0728(86)90123-3
[23] Z. Coldrick, P. Steenson, P. Millner, M. Davies, A. Nelson, Phospholipid monolayer coated microfabricated electrodes to model the interaction of molecules with biomembranes. *Electrochim. Acta* **2009**, *54*, 4954. doi:10.1016/J.ELECTACTA.2009.02.095
[24] Z. Coldrick, A. Penezic´, B. Gasparovic´, P. Steenson, J. Merrifield, A. Nelson, High throughput systems for screening biomembrane interactions on fabricated mercury film electrodes. *J. Appl. Electrochem.* **2011**, *41*, 939. doi:10.1007/S10800-011-0319-7
[25] S. W. Zhang, A. Nelson, Z. Coldrick, R. J. Chen, The effects of substituent grafting on the interaction of pH-responsive polymers with phospholipid monolayers. *Langmuir* **2011**, *27*, 8530. doi:10.1021/LA105125D
[26] N. Ormategui, S. W. Zhang, I. Loinaz, R. Brydson, A. Nelson, A. Vakurov, Interaction of poly(N-isopropylacrylamide) (pNIPAM) based nanoparticles and their linear polymer precursor with phospholipid membrane models. *Bioelectrochemistry* **2012**, *87*, 211. doi:10.1016/J.BIOELECHEM.2011.12.006
[27] S. P. Kounaves, J. Buffle, Deposition and stripping properties of

mercury on iridium electrodes. *J. Electrochem. Soc.* **1986**, *133*, 2495. doi:10.1149/1.2108457
[28] Z. Bi, P. Salau¨n, C. M. G. van den Berg, Study of bare and mercurycoated vibrated carbon, gold and silver microwire electrodes for the determination of lead and cadmium in seawater by anodic stripping voltammetry. *Electroanal.* **2013**, *25*, 357. doi:10.1002/ELAN.201200446
[29] M. M. Krahn, D. P. Herman, G. M. Ylitalo, C. A. Sloan,D.G. Burrows, R. C. Hobbs, B. A. Mahoney, G. K. Yanagida, J. Calambokidis, S. E. Moore, Stratification of lipids, fatty acids and organochlorine contaminants in blubber of white whales and killer whales. *J. Cetacean Res. Manag.* **2004**, *6*, 175.
[30] Y. Q. Tao, B. Xue, S. C. Yao, J. C. Deng, Z. F. Gui, Triolein embedded cellulose acetate membrane as a tool to evaluate sequestration of PAHs in lake sediment core at large temporal scale. *Environ. Sci. Technol.* **2012**, *46*, 3851. doi:10.1021/ES203102B
[31] R. H. Ke, Y. P. Xu, Z. J. Wang, S. U. Khan, Estimation of the uptake rate constants for polycyclic aromatic hydrocarbons accumulated by semipermeable membrane devices and triolein-embedded cellulose acetate membranes. *Environ. Sci. Technol.* **2006**, *40*, 3906. doi:10.1021/ES060493T
[32] Y. Q. Tao, S. Z. Zhang, Z. J. Wang, R. H. Ke, X. Q. Shan, P. Christie, Biomimetic accumulation of PAHs from soils by triolein-embedded cellulose acetate membranes (TECAMs) to estimate their bioavailability. *WaterRes.* **2008**, *42*, 754. doi:10.1016/J.WATRES.2007.08.006
[33] K. L. Li, C. A. Tihal, M. Guo, R. E. Stark, Multinuclear and magicangle-spinning nmr investigations of molecular-organization in phospholipid triglyceride aqueous dispersions. *Biochemistry* **1993**, *32*, 9926. doi:10.1021/BI00089A008
[34] H. Khandelia, L. Duelund, K. I. Pakkanen, J. H. Ipsen, Triglyceride blisters in lipid bilayers: implications for lipid droplet biogenesis and the mobile lipid signal in cancer cell membranes. *PLoS ONE* **2010**, *5*, e12811. doi:10.1371/JOURNAL.PONE.0012811
[35] D. Hellberg, F. Scholz, F. Schubert, M. Lovric, D. Omanovic, V. A. Hernandez, R. Thede, Kinetics of liposome adhesion on a mercury electrode. *J. Phys. Chem.B* **2005**, *109*, 14715. doi:10.1021/JP050816S
[36] W. E. May, S. P. Wasik, D. H. Freeman, Determination of solubility behavior of some polycyclic aromatic-hydrocarbons in water. *Anal. Chem.* **1978**, *50*, 997. doi:10.1021/AC50029A042
[37] H. B. Klevens, Solubilization of polycyclic hydrocarbons. *J. Phys. Chem.* **1950**, *54*, 283. doi:10.1021/J150476A011
[38] D. Mackay, W. Y. Shiu, Aqueous solubility of polynuclear aromatichydrocarbons. *J. Chem. Eng. Data* **1977**, *22*, 399. doi:10.1021/JE60075A012
[39] *Method 8270. Quantification of semivolatile organic compounds by gas chromatography/mass spectrometry (GC/MS)* **1993** (US Environmental Protection Agency: Washington, DC).
[40] A. Nelson, N. Auffret, J. Readman, Initial applications of phospholipid-coated mercury-electrodes to the determination of polynuclear aromatic-hydrocarbons and other organic micropollutants in aqueous systems. *Anal. Chim. Acta* **1988**, *207*, 47. doi:10.1016/S0003-2670(00)80781-3
[41] C. Rav-Acha, M. Rebhun, Binding of organic solutes to dissolved humic substances and its effects on adsorption and transport in the aquatic environment. *Water Res.* **1992**, *26*, 1645. doi:10.1016/0043-1354(92)90164-Y
[42] P. F. Landrum, S. R. Nihart, B. J. Eadie, W. S. Gardner, Reverse-phase separation method for determining pollutant binding to Aldrich humic-acid and dissolved organic-carbon of natural-waters. *Environ. Sci. Technol.* **1984**, *18*, 187. doi:10.1021/ES00121A010